Environmental Modelling & Software 24 (2009) 1182–1195

Contents lists available at ScienceDirect

Environmental Modelling & Software

journal homepage: www.elsevier.com/locate/envsoft

Dynamics of soil salinity in the Canadian prairies: Application of singular spectrum analysis

Igor V. Florinsky [a,*], Robert G. Eilers [b,1], Brian H. Wiebe [b], Michele M. Fitzgerald [c]

[a] Institute of Mathematical Problems of Biology, Russian Academy of Sciences, 4 Institutskaya St., Pushchino, Moscow Region 142290, Russia
[b] Land Resource Unit (Manitoba), Agriculture and Agri-Food Canada, 360 Ellis Bldg., University of Manitoba, Winnipeg, Manitoba R3T 2N2, Canada
[c] British Columbia Ministry of Agriculture and Lands, 200-1690 Powick Road, Kelowna, BC V1X 7G5, Canada

ARTICLE INFO

Article history:
Received 22 April 2008
Received in revised form
17 March 2009
Accepted 23 March 2009
Available online 25 April 2009

Keywords:
Time series analysis
Variability
Fluctuations
Oscillations
Monitoring
Electrical conductivity

ABSTRACT

We studied hidden periodicities and trends in the temporal dynamics of soil salinity in the Canadian prairies at a field scale. Singular spectrum analysis (SSA) was applied to time series of the groundwater depth (Dgw), total precipitation, groundwater electrical conductivity (ECgw), and soil electrical conductivity (ECe). We found that the temporal variability of soil salinity is determined by its seasonal and quasi-3-yr oscillations controlled by similar cycles of Dgw and ECgw, which are controlled by the precipitation. In the seasonal cycle, the system "precipitation – groundwater depth – groundwater salinity – soil salinity" proceeds as follows: The maximal level of the precipitation is reached in late May. The water table peaks 2 months after the maximal level of precipitation was reached. The seasonal oscillation of ECgw is in phase with that of Dgw. ECe peaks 1.5 months after the maximal level of ECgw was reached. In the quasi-3-yr cycle, ECe peaks about 14 months after the maximal rise of the groundwater. Most likely, this cycle of Dgw is a response to the 3-yr periodicity of the precipitation observed in the region. SSA is the effective tool to detect hidden oscillations in soil processes handling relatively short time series with missing records.

1. Introduction

Soil salinisation is a typical process for the Canadian prairies, the northern extension of open grasslands in the Great Plains of North America (Eilers et al., 1997). The origin of salinity in the prairies is related to the mineralogical composition of the soil parent material (Ballantyne, 1968), the underlying geological formations (Greenlee et al., 1968), and the hydrogeological systems (Henry et al., 1985). Sulphates of sodium, calcium, and magnesium dominate (Keller and van der Kamp, 1988).

Soil salinity is characterised by high temporal variability. However, trends and periodicities in temporal variability of soil salinity in the Canadian prairies remain unclear and conflicting. Harker et al. (1996) observed a fluctuation of soil salinity inversely related to annual precipitation. Ballantyne (1978) found that the changes in soil salinity might reverse direction from year to year, or may keep the same direction for several years and then reverse direction. Miller and Pawluk (1994) observed seasonal fluctuations in the salt concentration: it was low in the spring, whereas high in the summer and autumn. They attributed the periodicity to the increase of evapotranspiration in the growing season.

A deficit of appropriate data sets and application of improper tools are the reasons why the temporal variability of soil salinity has not been adequately investigated worldwide. To reveal temporal trends and periodicities of a process, one should (a) obtain a reasonably long time series describing the process, and (b) explore the data by a method of time series analysis. However, there is a lack of relatively long time series describing temporal dynamics of soil salinity. It has been commonly studied with data acquired at 2–10 temporal points (Chang and Oosterveld, 1981; Lesch et al., 1998; Corwin et al., 2006). In these cases, methods of time series analysis could not be applied due to the short lengths of the series, whereas descriptive statistics could not identify regularities in salinity dynamics. A few available relatively long time series of soil salinity were examined with descriptive statistics. This approach was successful when applied to records with a clear seasonality (Mondal et al., 2001), however, it failed to extract regularities in more complicated data (Ballantyne, 1978).

The objective of the study was to detect periodicities and trends in the temporal dynamics of soil salinity in the Canadian prairies at a field scale as a result of the interaction of climatic conditions,

* Corresponding author.
E-mail address: iflorinsky@yahoo.ca (I.V. Florinsky).
[1] Retired.

1364-8152/$ – see front matter © 2009 Elsevier Ltd. All rights reserved.
doi:10.1016/j.envsoft.2009.03.011

groundwater regime, and land use. We analysed an existing historical data set of the 8-years monitoring of a benchmark site. Data were processed by the singular spectrum analysis (SSA), a group of techniques predominantly used in geophysics to investigate hidden structure of time series (Elsner and Tsonis, 1996; Golyandina et al., 2001).

2. Study site

In 1988, seven long-term benchmark sites across the Canadian prairies was established to monitor and assess the dynamics of soil salinity due to changes in local climate conditions and groundwater regime, and to determine an influence of soil management on severity, extent, and dynamics of soil salinity. The most systematic data set has been collected at the Warren site (Fitzgerald and Eilers, 1999). It is located about 40 km northwest of the city of Winnipeg, Manitoba, Canada (50°08′ N, 97°38′ W) (Fig. 1a). A gravel road divides the site into the north and south portions. Both subsites measure 420 by 100 m, and the maximum relative relief is about 1 m (Fig. 1b) (Fitzgerald and Eilers, 1999).

The site is situated in the lacustrine Lake Manitoba Plain (Clayton et al., 1977), at an elevation of about 246 m above sea level. It is located within a continental climate zone with short, warm summers and long, cold winters. Mean annual temperature is

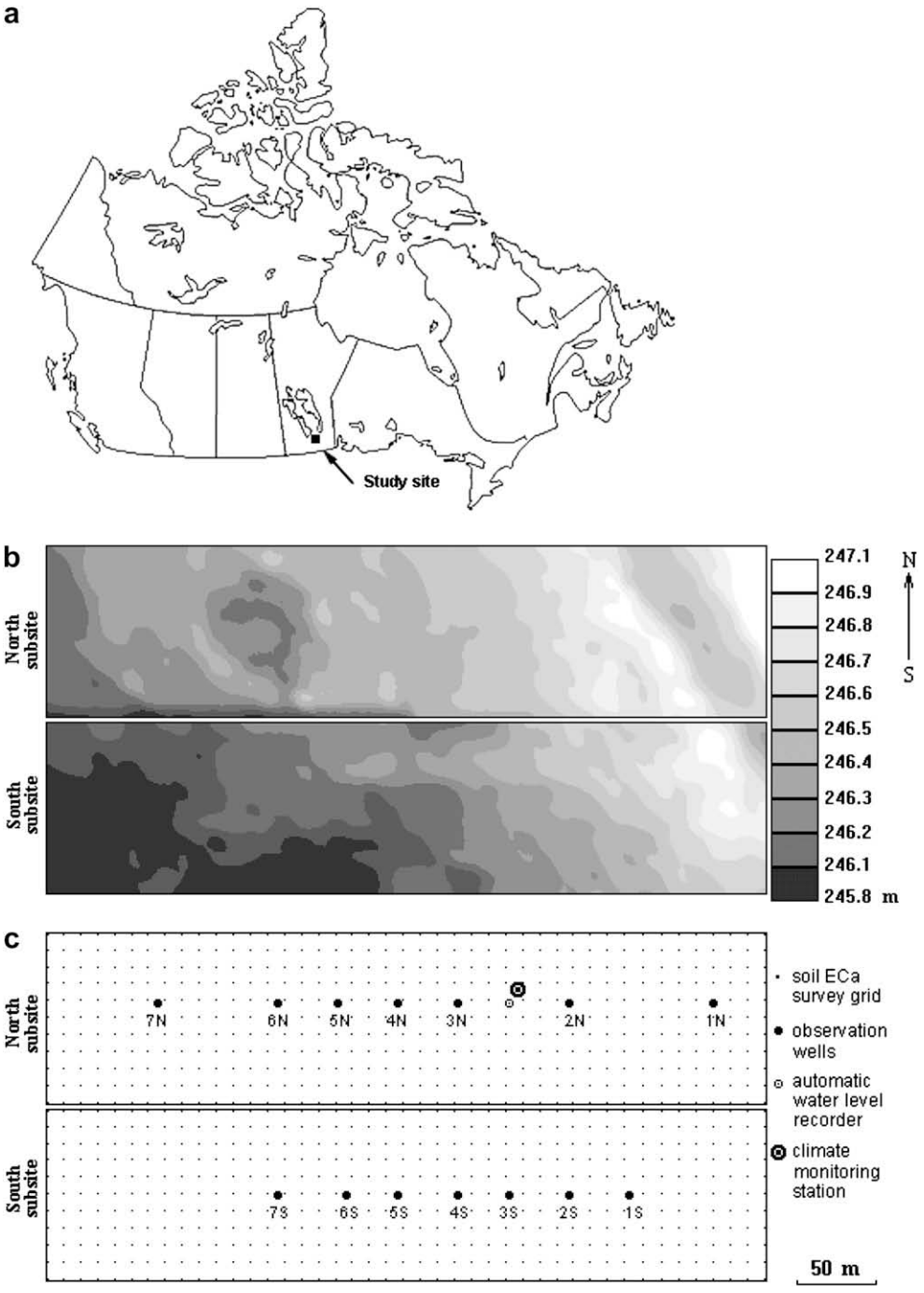

Fig. 1. The study site: (a) geographical position, (b) elevations, (c) monitoring design.

Table 1
Ionic concentrations (mg/L) in groundwater in wells at the north subsite on 20 July1992.

Ion	Well							
	1 N	2 N	Automatic water level recorder	3 N	4 N	5 N	6 N	7 N
Ca^{2+}	314	529	905	895	196	437	403	662
Mg^{2+}	448	2233	4465	4172	254	1626	1032	1755
Na^{+}	618	3428	3638	4243	582	1286	973	2431
HCO_3^-	366	1281	488	275	122	275	336	366
Cl^-	1750	8550	17,710	18,510	2020	4900	2970	9800
SO_4^{2-}	1065	8505	4308	4620	420	2001	1683	3888

2.1 °C, mean July temperature is 18 °C, mean January temperature is −18.3 °C. Mean annual precipitation is 545 mm including 350 mm as rainfall and 195 mm as snowfall. The average annual moisture deficit is approximately 200 mm, average growing season moisture deficit is about 260 mm.

The soil parent materials are moderately to strongly calcareous lacustrine clay to clay loam. The dominant soils are imperfectly drained Gleyed Rego Black Chernozems and imperfectly drained Rego Humic Gleysols with clay to clay loam surface textures (Soil Classification Working Group, 1998).

The site is located close to a near-northwest-striking hydraulic divide between fresh and saline water-bearing parts of the aquifer formed by a series of Middle Ordovician to Middle Devonian carbonates. Salinity on the site has originated from a slow discharge of saline groundwater from the aquifer. Average depth to the water table is 2 m. Mg^{2+}, Na^{+}, Cl^{-}, and SO_4^{2-} are the dominant ions responsible for groundwater and soil salinity on the study site (Table 1). Visible salt crusts and precipitates are common on the soil surface and in the soil profile, respectively.

The north subsite has been uncultivated since 1984. It was sod seeded to alfalfa in 1985. The south subsite has been deep-tilled annually and cropped by wheat, barley, and rapeseed since 1984.

3. Materials and methods

3.1. Data collection

Permanent grids were established on subsites with a 10 m interval (Fig. 1c). Using the grids, surveys of the electrical conductivity of the bulk soil (ECa) were done with a Geonics EM38 in the horizontal and vertical coil position (ECa_h and ECa_v, respectively). A pair of ECa_h and ECa_v measurements is used to estimate the ECa of a soil profile within depth increments of about 0–60 and 0–120 cm, respectively (Geonics Limited, 2005). Measurements of ECa_h and ECa_v were initiated in September 1991, repeated three times per year in 1992–1998 (in May, July, and September), and finished in May 1999, that is, 23 surveys were performed. Surveys were not conducted in late fall, winter, and early spring: differences in EM38 readings are obscure if soil temperature is below 0 °C (Woods and Hingley, 2004). In these seasons, the soil is frozen down to about 70 cm at the study site.

For each subsite, each EM38 survey included 473 measurements of both ECa_h and ECa_v. After each survey, data were calibrated. ECa depends on several factors other than soil salinity. Some of these factors are temporally dynamic, such as soil moisture. To eliminate influence of other factors, the calibration is mandatory (Rhoades et al., 1999). Five reference points were selected within each subsite to represent the range of ECa values of the particular survey, and to provide relatively uniform coverage across subsites (location of reference points has been varied from survey to survey). At each reference point, soil samples were collected at 0–30, 30–60, 60–90, and 90–120 cm depth increments. The electrical conductivity of the extract of a saturated soil-paste sample (ECe) was determined on each soil sample (Richards, 1954). For each reference point, the weighted ECe for the depth increments of 0–60 cm (ECe_h) and 0–120 cm (ECe_v) were calculated (Wollenhaupt et al., 1986):

$$ECe_h = 0.54 \times ECe_{0-30} + 0.26 \times ECe_{30-60} + 0.12 \times ECe_{60-90} + 0.08 \times ECe_{90-120}, \quad (1a)$$

$$ECe_v = 0.23 \times ECe_{0-30} + 0.35 \times ECe_{30-60} + 0.24 \times ECe_{60-90} + 0.18 \times ECe_{90-120}, \quad (1b)$$

where $ECe_{subscript}$ is ECe measured on a soil sample collected at the subscript depth increment. For each EM38 survey and for each subsite, ECe_h and ECe_v values were calculated for five reference points. For each survey and for each subsite, linear regression analyses of ECe_h against ECa_h, and ECe_v against ECa_v were carried out. Finally, for each EM38 survey, the regression equations obtained were used to convert all values of ECa_h and ECa_v to values of ECe_h and ECe_v, respectively (Table 2, Fig. 2).

Table 2
Summary statistics for ECe_h and ECe_v (dS/m).

Year	Month	The north subsite					The south subsite				
		min	max	$\bar{x}$	s	CV	min	max	$\bar{x}$	s	CV
1991	Sept.	1.04	20.13	8.58	4.46	52	0.01	22.78	4.53	4.22	93
		2.37	18.11	9.53	3.83	40	0.01	17.25	5.78	3.75	65
1992	May	1.03	19.64	8.85	4.36	49	0.79	21.43	7.14	3.62	51
		1.54	23.33	11.80	5.22	44	1.49	24.17	9.83	4.45	45
	July	1.60	17.07	7.61	3.46	45	0.01	24.22	5.04	4.20	83
		1.86	21.29	10.76	4.64	43	0.01	23.13	7.20	4.43	62
	Sept.	0.56	16.20	7.08	3.56	50	0.01	20.39	4.59	3.33	72
		0.78	21.23	10.56	4.89	46	0.01	21.79	6.69	4.18	63
1993	May	1.23	14.36	6.55	2.96	45	0.01	18.69	4.90	3.97	81
		1.47	15.68	8.02	3.27	41	0.01	18.85	6.14	4.25	69
	July	0.27	14.15	5.08	2.69	53	0.01	20.26	4.71	3.09	66
		0.23	14.79	6.85	3.39	50	0.46	18.28	6.23	3.17	51
	Sept.	0.01	13.16	5.15	2.88	56	0.01	23.63	5.20	3.85	74
		0.01	13.77	6.47	3.14	49	0.01	21.89	6.94	4.07	59
1994	May	0.01	30.30	9.85	6.59	67	0.01	35.99	7.90	5.86	74
		0.01	23.79	10.00	5.88	59	0.12	30.16	10.51	6.33	60
	July	0.01	26.34	9.55	5.71	60	0.01	26.63	6.92	4.38	63
		0.01	25.38	10.52	6.19	59	1.48	23.53	7.72	3.38	44
	Sept.	0.89	14.78	6.56	3.34	51	0.01	34.35	7.34	5.44	74
		0.55	15.90	7.34	3.62	49	0.01	28.01	7.95	4.91	62
1995	May	0.01	15.55	5.86	3.55	61	0.01	24.80	4.08	3.10	76
		0.01	17.09	7.22	4.08	57	0.38	14.84	5.75	2.83	49
	July	0.01	19.75	7.59	4.99	66	1.16	20.79	5.75	3.16	55
		0.01	22.53	9.27	5.33	58	0.85	18.11	6.46	3.14	49
	Sept.	0.01	13.02	5.55	3.18	57	0.01	21.05	5.51	3.75	68
		0.69	12.87	5.88	2.77	47	0.01	17.31	6.05	3.82	63
1996	May	0.01	14.83	5.75	3.35	58	0.01	23.46	5.76	3.78	66
		0.01	16.17	6.89	3.93	57	0.01	17.63	6.23	3.45	55
	July	0.01	16.16	5.60	3.38	60	0.06	20.59	5.88	3.58	61
		0.01	16.97	7.37	4.21	57	0.01	16.56	6.61	3.58	54
	Sept.	0.01	23.29	8.72	5.15	59	0.01	36.18	8.07	5.50	68
		0.59	21.18	9.89	4.74	48	0.01	24.46	9.56	5.02	53
1997	May	0.68	17.72	7.23	3.80	53	0.93	27.41	6.33	3.89	61
		0.01	17.51	7.41	3.84	52	0.01	23.65	8.68	4.75	55
	July	0.01	28.57	8.71	6.11	70	4.38	21.50	8.12	2.63	32
		0.01	17.05	7.19	4.02	56	1.41	19.40	8.57	3.92	46
	Sept.	0.51	20.91	8.60	4.58	53	0.36	20.79	6.58	3.82	58
		0.01	18.75	8.65	4.25	49	0.28	18.18	7.89	4.18	53
1998	May	0.68	18.72	6.47	3.35	52	0.85	23.18	5.85	3.00	51
		0.74	13.49	6.61	2.96	45	1.33	15.62	6.88	2.87	42
	July	0.75	20.77	7.42	3.77	51	0.66	23.39	6.46	3.38	52
		0.14	15.23	7.19	3.45	48	0.92	16.94	7.53	3.30	44
	Sept.	1.90	24.37	11.19	5.09	45	0.01	20.82	7.53	4.35	58
		0.83	22.80	11.18	4.90	44	1.05	13.86	7.40	3.02	41
1999	May	0.38	21.25	7.33	3.88	53	0.61	13.65	4.82	2.45	51
		0.46	18.54	9.02	4.30	48	0.84	12.19	5.47	2.38	43

ECe_h, upper values; ECe_v, lower values; max, maximal value; min, minimal value; $\bar{x}$, mean; s, standard deviation; CV, coefficient of variation.

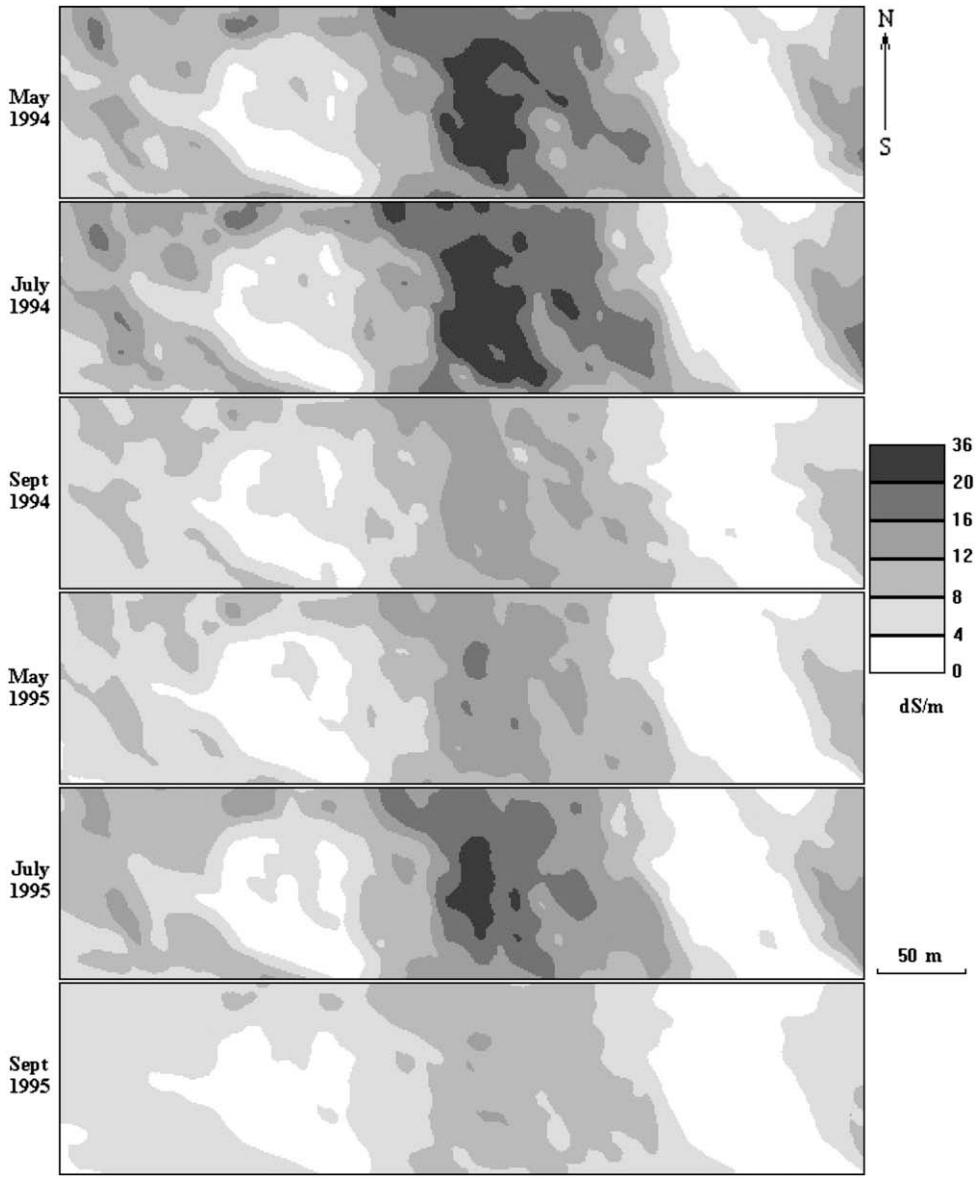

Fig. 2. Dynamics of the spatial distribution of ECe_v at the north subsite in 1994–1995.

A weather monitoring station CSI CR10 was installed on the site (Fig. 1c). The total rainfall has been measured from July 1991 until June 1999. A time series consists of 2922 daily records. For snowfall, we used records of the total precipitation from one of the closest weather stations (Delta Beach, Manitoba), where all snowfall has been converted to snow water equivalents. A time series of the monthly accumulative sums of the total precipitation consists of 96 records (Fig. 3a).

An automatic water level recorder Stevens Type F was installed at a shallow well on the site (Fig. 1c). The depth of groundwater level (Dgw) has been measured from July 1991 until June 1999. A time series of Dgw consists of 2922 daily records (Fig. 3b). Seven shallow observation wells were installed on each subsite along two transects across a microcatena (Fig. 1c). At wells, water sampling (about 1 time per month) was initiated in January 1992 and finished in December 1998. Samples were analysed for electrical conductivity (ECgw). There were 76 records of ECgw for each well (Fig. 3c).

3.2. Data processing

3.2.1. Preliminary treatment of data

Ideally, it would be desirable to measure ECe, Dgw, and ECgw at the same location(s) using a regular, monthly temporal interval. However, the ideal experimental design cannot be used since monthly measurements of ECa are impossible: the soil profile is frozen in winters (Section 3.1). Instead of an ideal data set of soil and groundwater parameters, there is the historical imperfect data set with missing records, which was collected for a different purpose within the frames of the long-term soil monitoring. To adopt the data to the peculiarities of SSA (Appendix A), we carried out a preliminary treatment of the data set:

1. ECe data sets were excessive: for each subsite, 23 data sets including 473 paired values of ECe_h and ECe_v each (Section 3.1). We restricted the analysis of ECe_v and ECe_h values to points near the observation wells, that is, 23 sets of seven points for each subsite. The microcatena is crossed by the well transects (Fig. 1b, c), so such a point selection served (a) to study the temporal variability of soil salinity respecting to slope position, and (b) to compare ECe with ECgw.
2. ECa measurements were not possible in cold seasons (Section 3.1). This lead to the generation of ECe time series with a varying step, which could not be treated by SSA. For the Canadian prairies, there are no data on behaviour of soil salinity in frozen soils. It is reasonable to suppose that soil salinity is not changing in a frozen soil. Therefore, an appropriate way to fill in missing records is to interpolate them from values for fall and spring. We applied a linear interpolation to generate time series with a bi-monthly step for ECe measured near wells. For each subsite, we obtained seven time series of both ECe_v and ECe_h consisting of 47 values each (Fig. 3d, e).
3. There were eight randomly missing records in ECgw data sets. To generate ECgw time series with a monthly time step, we used a linear interpolation. For each subsite, we obtained seven time series of ECgw consisting of 84 values each (Fig. 3c).

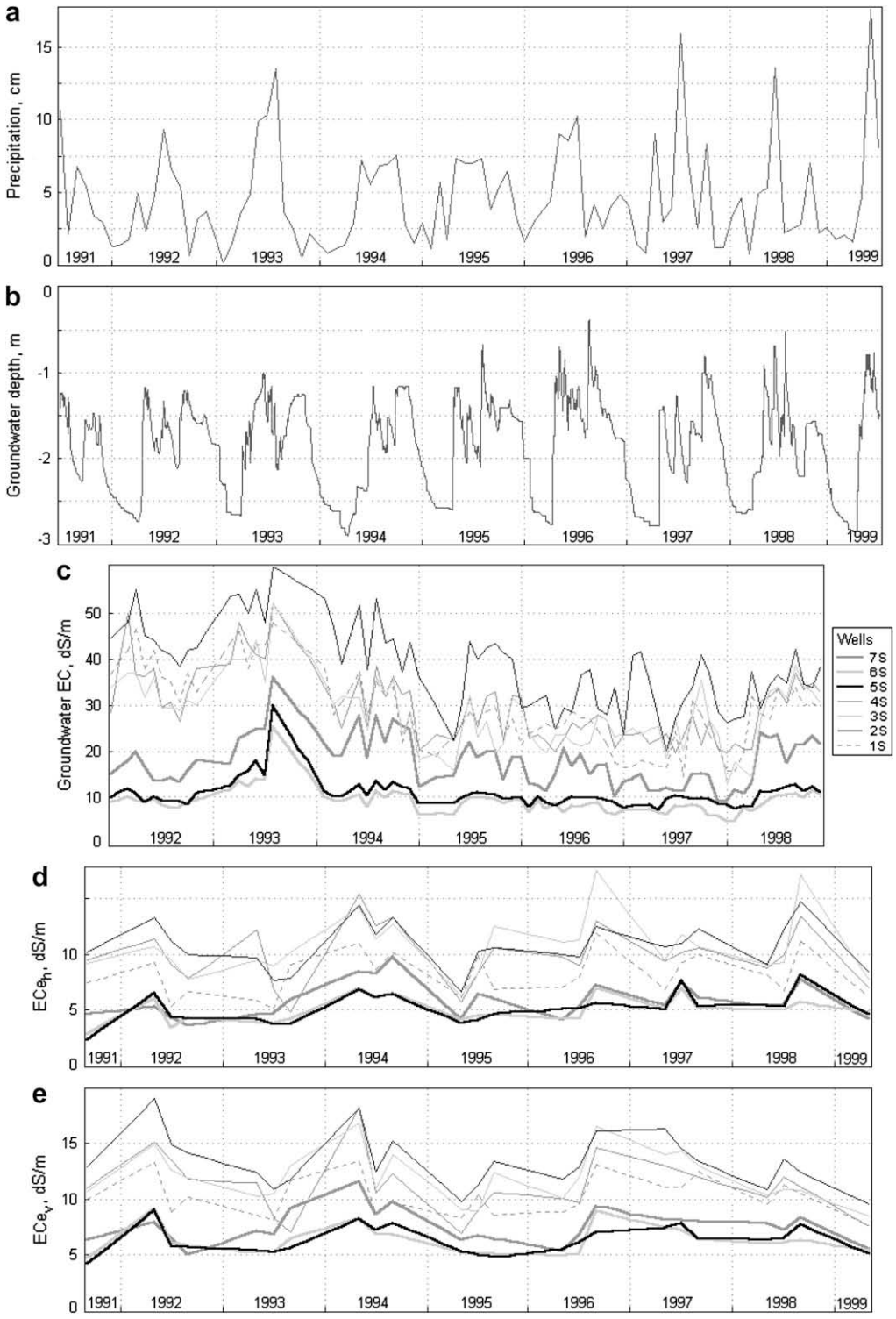

Fig. 3. Time series: (a) total precipitation; (b) depth to groundwater; (c) ECgw at the south subsite, wells 1S–7S; (d) ECe_h at the south subsite, wells 1S–7S; (e) ECe_v at the south subsite, wells 1S–7S.

4. We were interested in detecting common temporal regularities for all parameters under study. Therefore, although the temporal resolution of the Dgw series (daily records – Section 3.1) enabled one to search for oscillations with periods of several weeks, we did not do this analysis because the temporal resolution of ECgw and ECe series (monthly and bi-monthly steps, correspondingly) was inadequate to study short-term periodicities. The weekly step is sufficient to detect information contained in the Dgw time series (418 weekly records).
5. All time series were normalised.

3.2.2. Time series analysis

The following time series systems were treated by the multi-channel SSA (Appendix A):

- Seven time series of ECgw for both the north subsite and the south subsite (Fig. 3c);
- Seven time series of ECe_h for both the north subsite and the south subsite (Fig. 3d);
- Seven time series of ECe_v for both the north subsite and the south subsite (Fig. 3e).

Table 3
Parameters of times series, singular spectrum analysis, and periodicities revealed.

Time series	From	To	Step Δt	Length N	Window length L	Eigentriple pairs	Period of a harmonic	
							Average value, Δt	Rough value, month
Total precipitation	July 1991	June 1999	1 month	96	48	1–2	11.79	12
						16–17	19.27	19
Depth to groundwater	July 1, 1991	June 30, 1999	1 week	418	209	1–2	51.82	12
						3–4	26.19	6
						5–6	142.16, 19.00	33, 4.5
						7–8	19.00	4.5
						9–10	78.49	18
ECgw, the north subsite	Jan, 1992	Dec, 1998	1 month	84	24	2–3	12.20	12
ECgw, the south subsite	Jan, 1992	Dec, 1998	1 month	84	24	3–4	11.97	12
ECe_h, the north subsite	Sept, 1991	May, 1999	2 months	47	18	1–2	18.65	37
						4–5	8.68	17
ECe_h, the south subsite	Sept, 1991	May, 1999	2 months	47	18	1–2	17.77	36
						5–6	8.34	17
						3–4	5.87	12
ECe_v, the north subsite	Sept, 1991	May, 1999	2 months	47	18	2–3	11.75	24
						4–5	8.65	17
						6–7	3.36	7
ECe_v, the south subsite	Sept, 1991	May, 1999	2 months	47	18	1–2	18.03	36
						3–4	9.40	19
						5–6	5.88	12

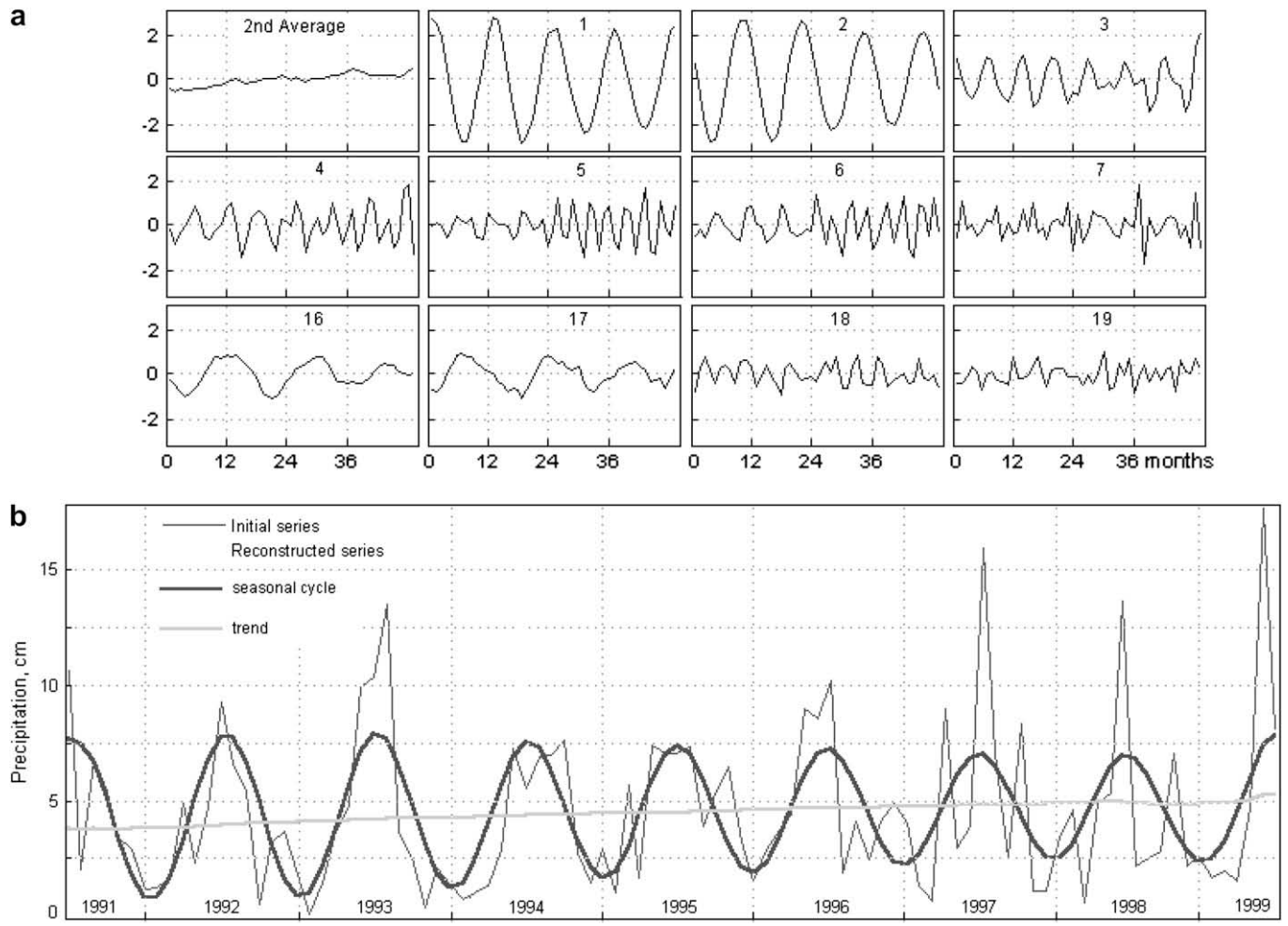

Fig. 4. The total precipitation: (a) graphs of some principal components (numbered, plotted on ordinates, dimensionless); (b) initial series and reconstructed series of the seasonal cycle and trend.

Time series of the total precipitation (Fig. 3a) and Dgw (Fig. 3b) were treated individually. Parameters of all time series are summarised in Table 3.

Converting one-dimensional time series into trajectory matrices, all time series were double-centred. As recommended, we tried several values of window length *L*. Selected values (Table 3) were the best concerning revealing regularities in the data. Principal components of time series were plotted as one-dimensional time series (Figs. 4a, 5a, 6a, 7a, and 8a). Two-dimensional graphs of eigenvectors were also constructed (e.g., Fig. 5b). They were visually analysed to select eigentriples related to periodicities and trends of initial time series. Eigentriples selected (Table 3) are discussed in Section 4.1. Finally, time series of periodicities and trends were reconstructed (Figs. 4b, 5c, 6b, 7b, and 8b) from eigentriples selected and related average components. Periodicities detected are summarised in Table 3. See Appendix A for details of SSA.

To analyse temporal interrelationships in the system "precipitation – groundwater depth – groundwater salinity – soil salinity", we plotted the first harmonics of the periodicities together: 12-month harmonics for seasonal cycles of the total precipitation, Dgw, ECgw, and ECe (Fig. 9a), and 36-month harmonics for 3-yr cycles of Dgw and ECe (Fig. 9b).

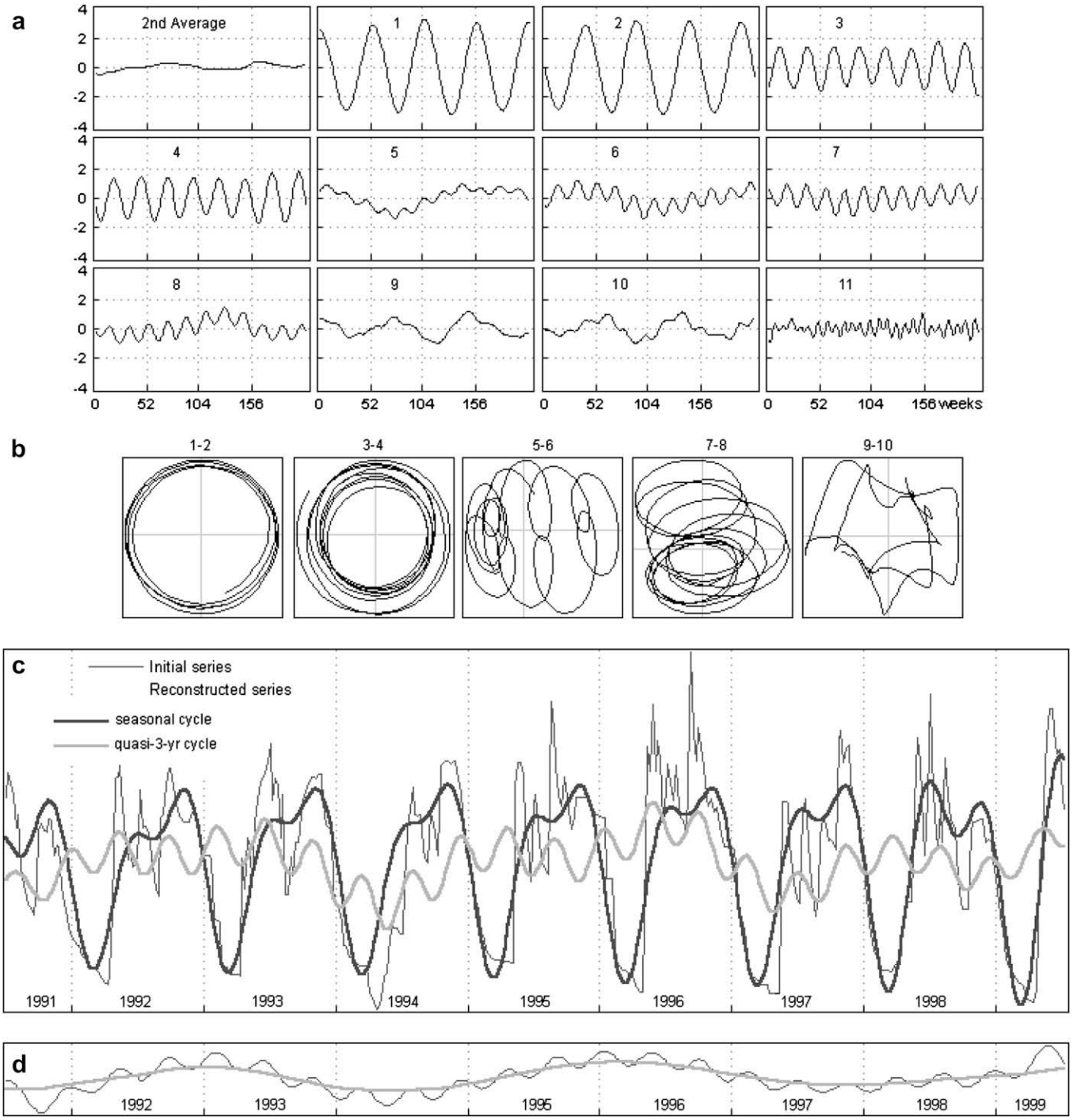

Fig. 5. The depth to groundwater: (a) graphs of some principal components (numbered, plotted on ordinates, dimensionless); (b) two-dimensional graphs of some eigenvector pairs (numbered); (c) initial series and reconstructed series of the seasonal and quasi-3-yr cycles; (d) a series generated from the eigentriples 5–6 and reconstructed series of the 36-months harmonic.

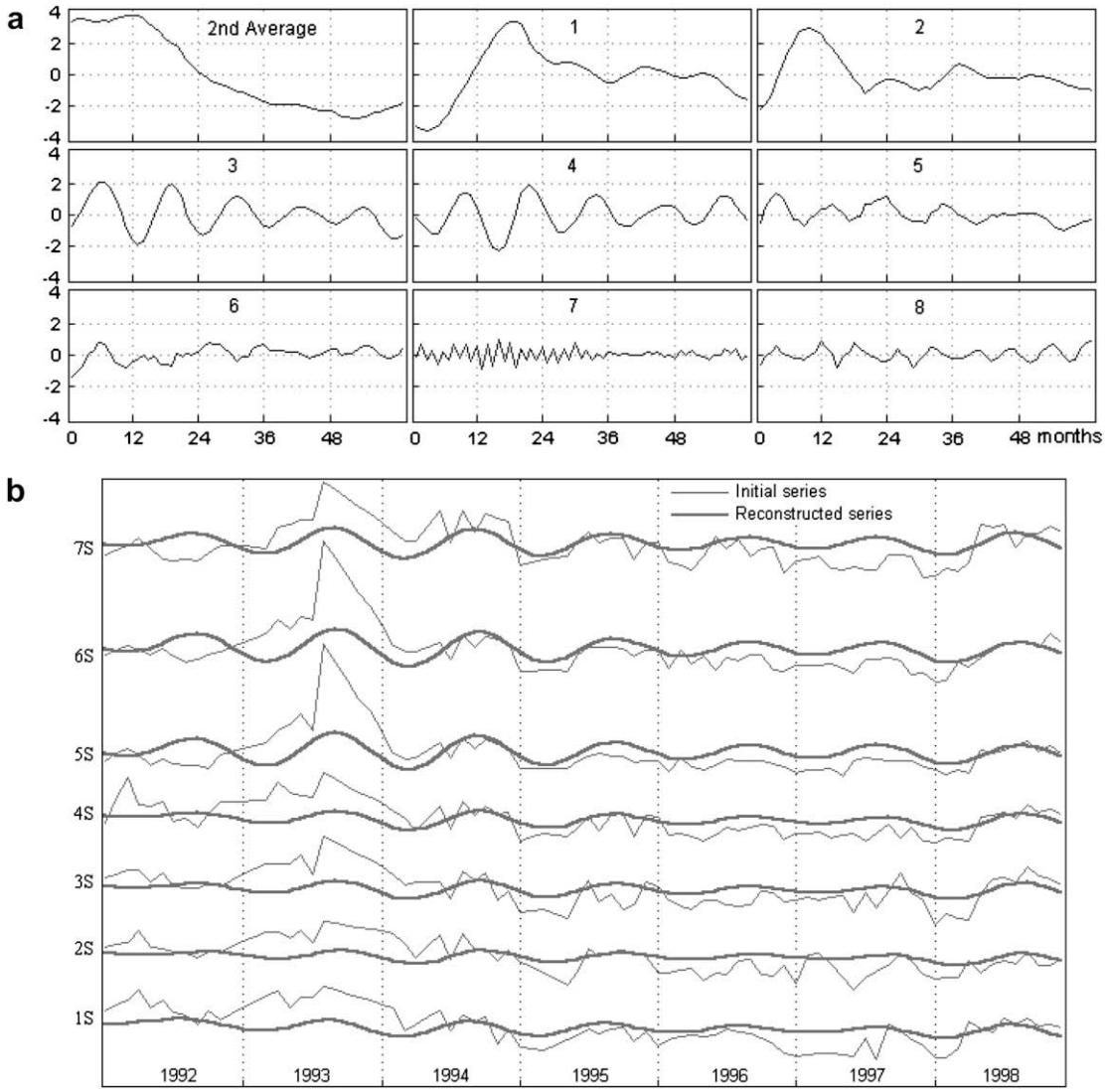

Fig. 6. ECgw at the south subsite, wells 1S–7S: (a) graphs of some principal components (numbered, plotted on ordinates, dimensionless); (b) initial series and reconstructed series of the seasonal cycle.

Graphs of initial and reconstructed series show normalised functions. Time series analysis was performed by software CaterpillarSSA 3.10 Professional M Edition (© GistaT Group, 1996–2001).

3.2.3. Statistical analysis

To evaluate an overall contribution of periodicities to the temporal dynamics of ECe_h and ECe_v, we carried out a linear correlation analysis between initial series of ECe_h and ECe_v at both subsites and related reconstructed series integrating all observed periodicities. Determination coefficients were also calculated. Analysis was done by Statgraphics Plus 3.0 (© Statistical Graphics Corp., 1994–1997).

4. Results and analysis

4.1. Eigentriples

For the precipitation, two periodicities were detected by the eigentriples 1–2 and 16–17 (Fig. 4a). They have average periods of about 12 and 19 months (Table 3), that is, these are the first harmonic of seasonal periodicity (Fig. 4b), and, probably, the second harmonic of a quasi-3-year periodicity. A trend (Fig. 4b) was identified by the second average component (Fig. 4a).

For Dgw, the eigentriples 1–2, 3–4, 5–6, 9–10, and 7–8 (Fig. 5a, b) identify five periodicities. They have average periods of ca. 12, 6, 33, 18, and 4.5 months, respectively (Table 3), that is, these are the first and second harmonics of seasonality (Fig. 5c), and the first, second, and fourth harmonics of a quasi-3-yr periodicity (Fig. 5c). The 4.5-months harmonic, identified by the eigentriples 7–8 is partly presented in the eigentriples 5–6 (Fig. 5a). This is a case of "weak separability": a sum of two sines with similar amplitudes, but different periods generates four equal eigenvalues blending the sines (Golyandina et al., 2001). To extract a pure 36-months harmonic of Dgw, we performed a double processing of the initial series. First, we reconstructed a series from the eigentriples 5–6 of the initial series of Dgw. Then, we decomposed this reconstructed series with $L = 52$. Finally, we reconstructed the required harmonic from the average components of the second decomposition (Fig. 5d).

For ECgw at the south subsite, a periodicity was detected by the eigentriples 3–4 (Fig. 6a). This is the first harmonic of seasonality (Fig. 6b) since its average period is 11.97 months (Table 3). The similar regularity was detected for ECgw at the north subsite (Table 3).

For ECe_h at the south subsite, three periodicities were identified by the eigentriples 1–2, 5–6, and 3–4 (Fig. 7a). They have average

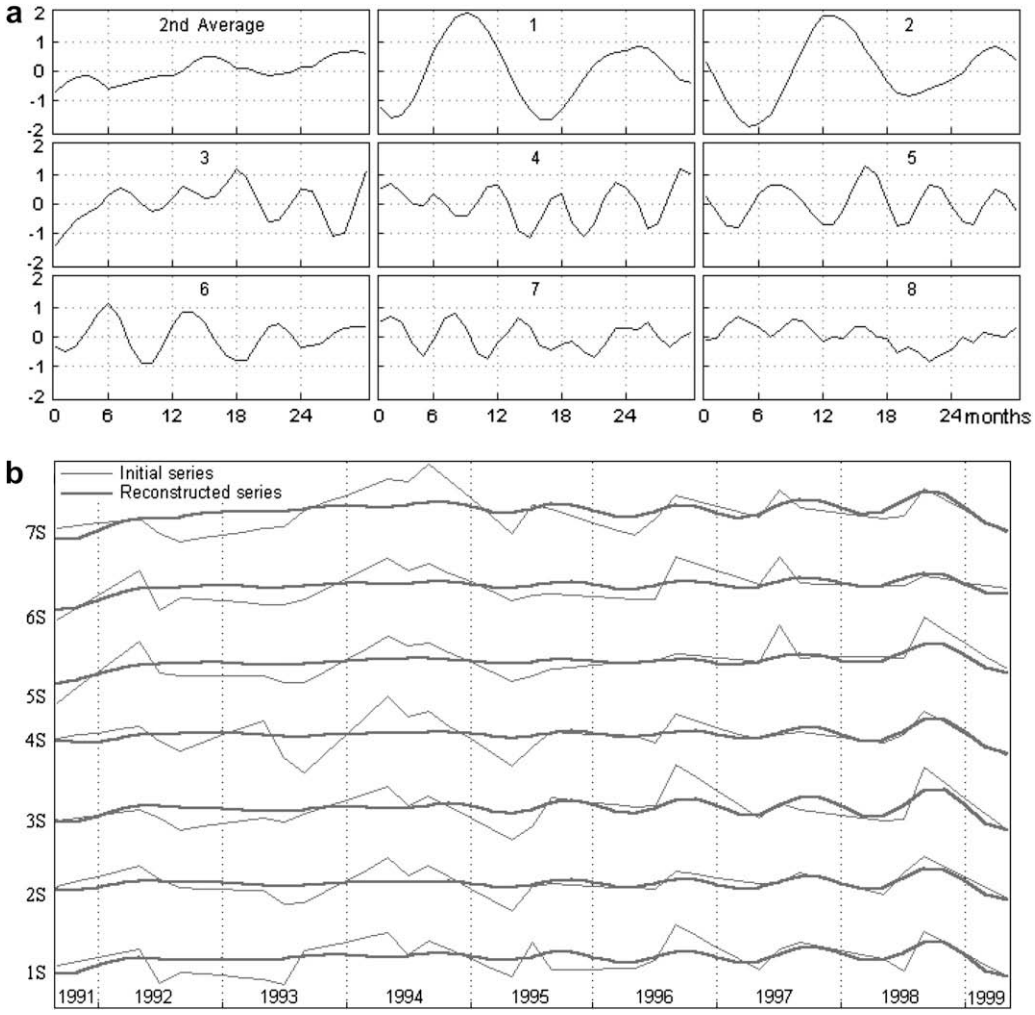

Fig. 7. ECe_h at the south subsite, wells 1S–7S: (a) graphs of some principal components (numbered, plotted on ordinates, dimensionless); (b) initial series and reconstructed series of the seasonal cycle.

periods of about 36, 17, and 12 months, respectively (Table 3), that is, they are the first and second harmonics of a quasi-3-yr periodicity, and the first harmonic of seasonality (Fig. 7b). A trend was detected by the second average component (Fig. 7a). Similar harmonics of a quasi-3-yr periodicity were found for ECe_h at the north subsite (Table 3).

For ECe_v at the south subsite, three periodicities were revealed by the eigentriples 1–2, 3–4, and 5–6 (Fig. 8a). They have average periods of ca. 36, 19, and 12 months, correspondingly (Table 3), that is, these are the first and second harmonics of a quasi-3-yr periodicity (Fig. 8b), and the first harmonic of seasonality. For ECe_v at the north subsite, three periodicities were revealed by the eigentriples 2–3, 4–5, and 6–7 (average periods are ca. 24, 17, and 7 months, respectively – Table 3).

4.2. Oscillations of soil salinity

Application of SSA allowed us to detect the following periodicities:

- The ordinary, marked seasonal cycle of the total precipitation (Fig. 4b);
- The pronounced seasonal and quasi-3-yr cycles of Dgw (Fig. 5c, d);
- The seasonal cycle of ECgw at both of subsites (Fig. 6b);
- Weak seasonal cycles of ECe_h and ECe_v beginning in 1995 at the south subsite (Fig. 7b);
- Quasi-3-yr cycles of ECe_h and ECe_v at the south subsite and ECe_h at the north subsite (Fig. 8b).

Existence of the following periodicities was also evidenced by their second harmonics:

- The quasi-3-yr cycle of the total precipitation;
- The quasi-3-yr cycle of ECe_v at the north subsite.

The seasonal and quasi-3-yr cycles are governing factors in the temporal variability of soil salinity. Indeed, integral reconstruction of two revealed cycles could explain up to 88% of the temporal variability in ECe (Table 4). The integration of periodicities gave a better fit to ECe at the south subsite. Residuals are caused by high-frequency natural events influencing soil salinity and errors of ECa measurement and calibration, and ECe interpolation.

In the seasonal cycle, the system "precipitation – groundwater depth – groundwater salinity – soil salinity" proceeds as follows (Fig. 9a). The maximal level of the precipitation is reached in late May – early June. The maximal rise of the water table is reached in

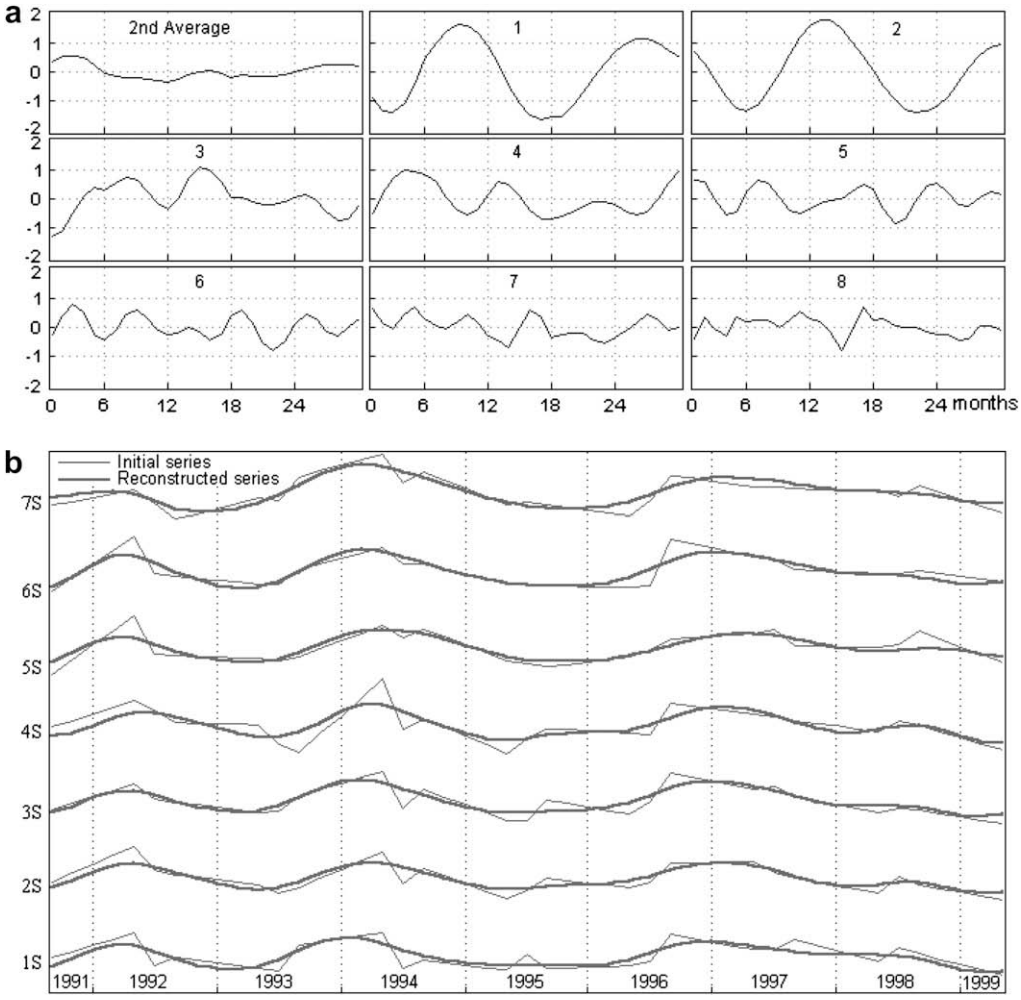

Fig. 8. ECe_v at the south subsite, wells 1S–7S: (a) graphs of some principal components (numbered, plotted on ordinates, dimensionless); (b) initial series and reconstructed series of the 3-yr cycle.

August, that is, about 2 months after the precipitation peaked. The seasonal oscillation of ECgw is in phase with the seasonal oscillations of Dgw: the higher shallow water table, the higher groundwater salinity. Beginning in 1995, the soil salinity peaks in the late September, that is, approximately 1.5 months after the maximal ECgw was reached. The mutual arrangement or phases of the seasonal cycles of the precipitation, groundwater depth, groundwater salinity, and soil salinity are constant.

Seasonal periodicities of the precipitation and Dgw of these sorts are ordinary for the Canadian prairies. Annual fluctuations of Dgw are caused by the seasonal recharge of aquifers: there is a rise of the groundwater level in early summer as a response to snow melting and rains in spring (Van der Kamp and Maathuis, 1991). The seasonal increase of ECe responding to the seasonal rise of Dgw and increase of ECgw is obvious: (a) the deeper the saline groundwater, the less upward migration of salt from the groundwater, and the less soil salinity, and (b) the higher the salinity of the groundwater, the higher the soil salinity for a given groundwater depth (Corwin et al., 1989). However, the seasonal rise of Dgw and the seasonal increase of ECgw go on simultaneously. This fact suggests that the seasonal rise of the groundwater level, following the seasonal maximum of precipitation, is caused by an influx of more saline groundwater, rather than by fresh meteoric waters in themselves. A possible cause of this effect is discussed in the next section. A gradual intensification of the ECe seasonality (Fig. 7b) might be connected with the progressive increase of the total precipitation (Fig. 4b).

In the quasi-3-yr cycle, the soil salinity peaks about 14 months after the maximal rise of the groundwater (Fig. 9b). The time delay was 15–17 months in 1993–1994, and 12–13 months in 1996–1997. We detected only the second harmonic for the 3-yr periodicity in the precipitation (Section 3.2.2), and we did not find a 3-yr cycle for ECgw. This may be caused by unsatisfied accuracy and temporal resolution of the time series. The lack of information can be compensated by previous observations. For the fresh water-bearing portion of the carbonate aquifer located 25–60 km east and southeast of the study site, Chen et al. (2004) found that (a) there are 3-yr cycles of the precipitation and Dgw (origin of the precipitation cycle is unknown); (b) there is a delay of 1–2 years in responses of the watertable level to changes of the precipitation. It is doubtful if different medium-term regularities in the precipitation occur within the same region. In addition, the carbonate aquifer under discussion is a unified system (Grasby and Betcher, 2002), so medium- and long-term fluctuations of the watertable level in its fresh water-bearing portion may be transmitted to the saline water-bearing portion. Thus, we suppose that the quasi-3-yr cycle of Dgw observed on the study site is a response to the 3-yr cycle of the precipitation found in adjacent areas. Although a 3-yr periodicity in ECgw was not detected, it might be the coupling agent between the quasi-3-yr cycles of Dgw and ECe (Fig. 9b).

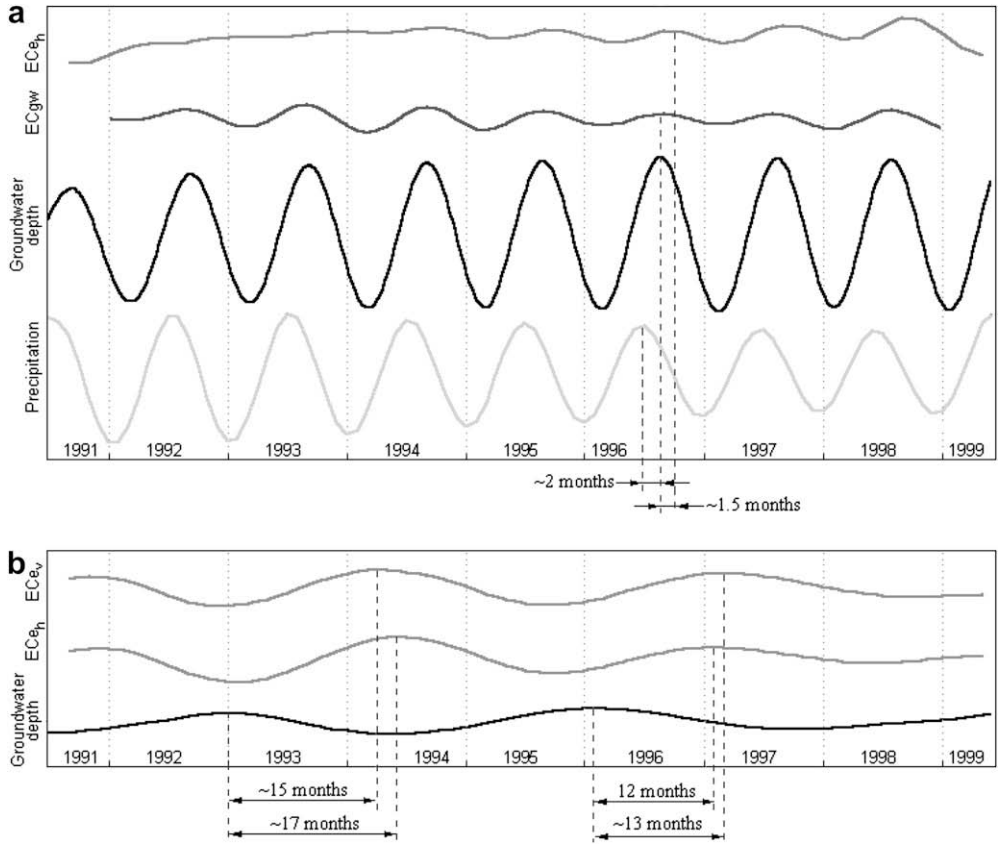

Fig. 9. Relationships between oscillations of the total precipitation, Dgw, ECgw, and ECe at the well 7S: (a) the seasonal cycle, (b) the 3-yr cycle.

There are no trends in time series of the Dgw, ECgw, ECe_v, and ECe_h at the north subsite. This testifies that these variables describe "stationary" processes, at least over the course of the monitoring. There is a weak, linear increase in the precipitation (12 mm per eight years – Fig. 4b). At the south subsite, there is gradual, almost linear increase in ECe_h by 1 dS/m per eight years.

We should note that although SSA reveals hidden periodicities, in general, SSA does not validate them for a single time series in the absence of model. However, our results can be considered as validated since the two cycles were revealed in the whole set of time series, which describe different natural processes and were collected with different methods and devices. We suppose that the found regularities can be typical for salt-affected (agro) landscapes of Canadian prairies marked by the similar natural conditions.

4.3. Spatial regularities of soil salinity

Maps of ECe_h and ECe_v show pronounced spatio-temporal changes of soil salinity (Fig. 2). However, the main spatial patterns of salinisation remain constant: the most salt-affected zone relates to a mid-slope position (Fig. 1b), while up- and down-slope positions are less affected. This is in agreement with previous observations: since depressions have additional moisture due to overland runoff, they have more leached soils than slopes and crests. As a result, at a field scale, saline soils are typical for slopes around depressions through redistribution and secondary accumulation of leached salts (Ballantyne, 1963; Stolte et al., 1992; Miller and Pawluk, 1994).

At each instant of time, values of soil and groundwater electrical conductivities diverge considerably at different landscape positions (Figs. 2 and 3c–e). However, comparing the reconstructed series of ECgw, ECe_h, and ECe_v related to different wells, one can see that seven time series share a common behaviour within each data set (Figs. 6b, 7b, and 8b). Therefore, there is no dependence of the temporal dynamics of soil and groundwater salinity on relief (e.g., displacements in phase, or better/worse manifestation of periodicities at distinct landscape positions).

Subsites show distinctions in soil salinisation. First, the north grassed subsite has a higher level of soil salinity than the south cultivated subsite (Table 2). Second, the north subsite is marked by

Table 4
Correlation coefficients between initial and reconstructed series (integration of two periodicities revealed) and determination coefficients.

Parameter	Well								
	1	2	3	4	5	6	7	Mean correlation	Mean determination
ECe_h, the north subsite	0.85	0.80	0.88	0.86	0.84	0.84	0.83	0.84	0.71
ECe_h, the south subsite	0.86	0.91	0.90	0.88	0.84	0.88	0.94	0.89	0.79
ECe_v, the north subsite	0.87	0.74	0.81	0.75	0.80	0.74	0.80	0.79	0.62
ECe_v, the south subsite	0.89	0.92	0.92	0.90	0.92	0.92	0.94	0.91	0.83

Significance level of all correlation coefficients is 0.00.

weaker oscillations of salinity: (a) seasonal cycles of ECe_h and ECe_v were not detected; and (b) only the second harmonic of the quasi-3-yr cycle of ECe_v was detected. Third, there are "anomalous" 24- and 7-months harmonics of ECe_v at the north subsite (Table 3), which are apt to be a distortion of the dominant periodicities revealed. Causes of the effects are discussed in the next section.

5. Discussion and conclusions

5.1. Oscillations of soil salinity

In the area under study, the temporal variability of soil salinity is formed by its seasonal and quasi-3-yr cycles controlled by similar cycles of the groundwater depth and salinity, which in turn are caused by related periodic impulses of the precipitation. The 3-yr cycle prevails. The interaction of the seasonal and 3-yr cycles leads to the intricate overall picture of the temporal dynamics of salinity.

Distinct manifestation of two cycles of different origin (the seasonality controlled by the revolution of the Earth around the Sun, and the 3-yr cycle of unknown genesis) illustrates a hierarchical concept reasoning that processes of different origin, as a rule, correspond to different spatial and/or temporal scales (Wagenet, 1998; MacDonald and Case, 2000). The potent and relatively frequent seasonal oscillation of the groundwater level has caused a near prompt, but relatively weak response of the soil salinity (Fig. 9a). The gradual and relatively rare influence of the 3-yr oscillation of the watertable level has led to the delayed, but relatively pronounced response of ECe (Fig. 9b). The distinct responses of the soil may reflect a "buffering" effect of soil capillary processes.

The seasonal concurrent increase of the watertable level and the shallow groundwater salinity may be explained as follows. The meteoric water moving through the clay and silty/sandy loam soils of the top metre of the profile may dissolve salts present there and impact the near surface groundwater. There is the potential for the salinised meteoric water to move laterally through the silt/sand loam layer marked by relatively high hydraulic conductivity, increased by desiccation cracks and biopores, and impact areas of lower salinity with salts from more saline areas.

It is anticipated that climate change may cause aridisation of the Great Plains in Canada in this century (Saunders and Byrne, 1994; Gan, 1998). Aridisation of grasslands may lead to a fast and pronounced decline of groundwater level, an increase of moisture deficit and soil salinisation, and salinisation of shallow groundwaters and surface waters. To handle these probable effects, there is a need to gain a better insight into climate and hydrological variations in the prairies as well as the dynamics of soil salinity there. Although the 8-years of monitoring provided us with reasonable data to identify medium-term cycles of the soil salinisation, the data are not adequate to detect its long-term oscillations and trends. Harker et al. (1996) concluded that even a 55-yr period is too short to reveal trends in soil salinisation. Indeed, periodicities of climate changes in this region correspond to the 18.6-yr lunar nodal cycle and the 11-yr solar cycle (Currie, 1984; Currie and O'Brien, 1990).

5.2. Soil salinity and land use

Our results suggest that dissimilar land use differently modulates spatio-temporal properties of soil salinisation: salinity is higher at the north uncultivated grassed subsite, but salinity oscillations are more pronounced at the south subsite, which is annually tilled and cropped. Perhaps, the source of the differences is the impact of annual cropping versus perennial forage. Annual cereal crops have their highest water requirements from jointing to the soft dough stage, which in most years would be the month of July. By mid-August, the water demand of a cereal crop is low. Alfalfa uses available water throughout the growing season and has the potential to use much more water than a cereal crop. Therefore, under identical groundwater and precipitation conditions, we would expect the following:

- Compared to the south subsite, the north subsite has drier root zone in June, August, and September and hence less likelihood of salt migration into the root zone or to the soil surface.
- At the south subsite, the water demand of cereal crop is low when precipitation is the highest (May–June) and hence there could be more leaching of salts at this time. At the north subsite, the crop uses more precipitation and less meteoric water leaches below the root zone.
- At the south subsite, as the annual cereal matures and water use declines, Dgw is peaking and more salt can be carried to the surface by capillary rise and hence the elevated groundwater levels may have a larger impact on ECe_v and ECe_h.

The result would be a much more pronounced oscillation in soil salinity for the south subsite than for the north one: the annual cereal cropping system can cause more favourable conditions for leaching of salts in late spring and for capillary migration of soluble salts from the groundwater to the soil surface in August and September than would the perennial forage cropping system.

There are two recommended management practices for moderate to severe soil salinity: minimising tillage and establishing a permanent vegetative cover (Halvorson, 1990). Permanent vegetation promotes infiltration (leaching), whereas tillage promotes exfiltration (salinisation). This raises the question of whether zero-tillage stabilises or reduces the severity and extent of soil salinity on the site. The lack of trends in the north subsite infers that salinisation has been stabilised, whereas on the south subsite, a weak trend for increasing soil salinity is correlated with continuous cultivation.

The natural cycles are largely independent of land use practices. A practice may modulate the manifestation of a cycle, but the cycle itself is independent until the practice begins to affect the driving force of the cycle. Therefore, one may either ignore cycles in soil management, or adjust the land use practice to them. The latter may improve the land use sustainability. In the case of soil salinity, one may ignore its natural periodicities and use zero-tillage because the relatively stabilised soil salinity requires, more or less, a uniform practice. However, the stabilised salinity may be rather high depending on (hydro) geologic conditions. If one prefers to use conventional tillage, there is an option to consider detected periodicities of soil salinity: amounts of manure applied may be varied depending on the year, or salt tolerant plants may be cropped in the most salt-affected years.

5.3. SSA – a tool to analyse soil data

The importance of oscillating processes cannot be overstated. During the course of evolution, the ability to "survive" is unique to oscillating systems (Molchanov, 1967). "Stable" inflexible systems turn into inert parts of the environment, whereas unstable systems collapse. For soils, these trends may be interpreted as follows:

- Evolution of soils exhibiting exo- and/or endogenous oscillations in soil physical, chemical, and biological processes;
- Gradual conversion of soils into bedrocks if soil oscillating processes were terminated for one reason or other (e.g., buried soils); and
- Collapse or degradation of soils being in an unstable state for a relatively long time.

Detection of oscillations in soil processes is particularly critical to model soil evolution. Three natural cycles are recognised in soil science: (a) the diurnal short-term periodicity in soil temperature and soil moisture modulated by diurnal rhythms of the insolation and air temperature (Menziani et al., 2003; Seybold et al., 2002); (b) the semidiurnal short-term periodicity in soil pH and soil redox potential modulated by semidiurnal tidal-driven fluctuations of the groundwater level (Seybold et al., 2002); and (c) the circannual medium-term periodicity modulated by circannual rhythms of the solar radiation, air temperature, and precipitation (Laio et al., 2002; Seybold et al., 2002; Miller et al., 2007). All three cycles are exogenous: diurnal cycles are governed by the Earth's rotation, semidiurnal cycles are controlled by the gravitational interaction in the system "Sun–Earth–Moon", whereas the Earth's revolution around the Sun is responsible for circannual cycles. Little else has been reported regarding other periodic fluctuations in soil properties. The exception was a study by Chudinova et al. (2006) reported several medium-term cycles of the soil temperature related to air temperature fluctuations in the Northern Eurasia (e.g., 2.7-yr, 4.3-yr, and 7.7-yr cycles). Thus, our paper described one of the first research on soil oscillating processes exhibiting a medium-term periodicity other than circannual. Notice that Chudinova et al. (2006) also mined data with SSA.

SSA is a free-of-model, nonparametric approach, viz. it is intended for cases, when a nature of a time series is unknown. Compared to conventional techniques of time series analysis, SSA reveals the same trends and high-frequency oscillations, but it is more advantageous to detect relatively weak and low frequency oscillations. Other merits of SSA are: (a) relatively short time series can be successfully analysed; (b) there is no need to transform nonstationary time series; and (c) inherent interactivity of the method provides a high level of flexibility in data analysis (Danilov and Zhigljavsky, 1997; Golyandina et al., 2001).

The application of SSA to time series of soil and groundwater salinity demonstrated its potential to reveal hidden temporal regularities in relatively short and rough time series. Investigation of temporal variability of soil processes is one of key problems of soil science (Heuvelink and Webster, 2001). As a rule, a long-term soil experiment is a cumbersome and expensive procedure. Sometimes, careful soil monitoring is made difficult by severe climatic conditions. Therefore, time series properly describing dynamics of soil properties are not easily accessible. As a result, one would have to handle historic data with missing records and irregular temporal sampling intervals. SSA offers an opportunity to study the temporal domain of soil processes, specifically oscillating processes in soils.

Acknowledgements

The authors are grateful to the King and Gallant families for allowing us to work on their fields, D. Swidinsky (Manitoba Land Resource Unit, Winnipeg, Canada) for the field and laboratory assistance, N.E. Golyandina (Department of Statistical Modelling, St.-Petersburg State University, Petrodvoretz, Russia) for useful advices, and two anonymous reviewers for helpful criticism. The study was partially supported by Agriculture and Agri-Food Canada, and the Department of Soil Science, University of Manitoba, Winnipeg, Canada.

Appendix A. Principles of SSA

Consider a time series $F_N = (f_0, f_1, \ldots, f_{N-1})$ of length N as a sum of additive components (i.e., a trend, periodicities, and noise). To extract an additive component S_N of the time series $F_N = S_N + R_N$, R_N is a residual, the basic version of SSA consists of four main steps (Golyandina et al., 2001). The first step includes selection of a window length L, an integer, $1 < L < N$, and construction of a trajectory matrix $\mathbf{X}$ with L-lagged vectors $X_j = (f_{j-1}, \ldots, f_{j+L-2})^{\mathrm{T}}$ as columns, T represents the transpose, $j = 1, \ldots, k$, $k = N - L + 1$. The second step is calculation of the matrix $\mathbf{XX^T}$ and its eigenvalues and eigenvectors ordered by decreasing the eigenvalues. The eigentriples (eigenvalues, eigenvectors, and principal components) form a singular value decomposition (SVD) of the matrix $\mathbf{X}$. The third step is identification of a group I of eigentriples corresponding to S_N and calculation of the grouped matrix $\mathbf{X^I}$ by summation of the corresponding SVD components. The fourth step includes reconstruction of the component $\tilde{S}_N$ calculated by diagonal averaging of the matrix $\mathbf{X^I}$.

Selection of L value depends on the problem under study and *a priori* information on the time series. If the time series has a periodicity with a known period, it is well to select L in proportion to the period since this leads to a "resonance" effect. It is advisable to try several L values.

The version of SSA with double centring contains the preliminary step: the SVD is produced for a matrix $\mathbf{X}^* = (x_{ij}^*)_{i,j=1}^{k,L}$, which is derived from the matrix $\mathbf{X}$ by double centring by both rows (the first averaging) and then columns (the second averaging), $x_{ij}^* = x_{ij} - \bar{x}_{i\cdot} - (\bar{x}_{\cdot j} - \mu)$, $\bar{x}_{i\cdot} = (1/k)\sum_{j=1}^{k} x_{ij}$, $\bar{x}_{\cdot j} = (1/L)\sum_{i=1}^{L} x_{ij}$, $\mu = (1/kL)\sum_{i=1}^{k}\sum_{j=1}^{L} x_{ij}$.

Principal components and eigenvectors are plotted as one-dimensional time series (e.g., Fig. 4a) and two-dimensional graphs (pairs of principal components or eigenvectors are plotted along x- and y-axes – e.g., Fig. 5b). Identification of an eigentriple group I can be done by a visual analysis of such graphs. For example, trend components can be found on one-dimensional graphs of principal components and eigenvectors. Double centring produces two average components. For a relatively small window length, the first average can be considered as a constant value (a shift along Y-axis), whereas the second average represents a trend (e.g., the second average component in Fig. 4a).

A periodical component of the time series produces a pair of approximately equal eigenvalues, a pair of periodical eigenvectors, and a pair of periodical principal components of the same period. To identify a periodical component of the time series, there is a need to find a pair of similarly oscillating eigenvectors, their eigenvalues and pair of principal components. These can be visually found on one-dimensional graphs of principal components and eigenvectors (e.g., the principal components 1 and 2 in Fig. 5a). Two-dimensional graphs are used to search for a pair of similarly oscillating functions: a harmonic with an integer period is displayed as a regular polygon, whereas a spiral is displayed if the amplitude of a harmonic is changed. Although "ideal" figures may be produced from real data (e.g., the eigenvectors 1–2 in Fig. 5b), attention should be given to quasi-regular figures.

Noise components of the time series can be found as high-frequency principal components and eigenvectors with beating amplitudes (e.g., the principal component 7 in Fig. 6a).

SSA can be used to analyse a system of time series $\{f_i^{(p)}\}_{i=0}^{N-1}$, where $p = 1, \ldots, d$; d is a number of time series in the system, or a dimension of a multi-dimensional sample, N is a number of elements in a time series (see the algorithm elsewhere – Elsner and Tsonis, 1996). The system may describe various processes measured in different units for the same temporal interval with the same temporal step. Each principal component k in length is common for all time series, whereas each eigenvector consists of p parts L in length related to a particular time series. This provides the possibility to find common features in different time series, and to reconstruct distinct manifestations of common regularities in different time series.

References

Ballantyne, A.K., 1963. Recent accumulation of salts in the soils of southeastern Saskatchewan. Canadian Journal of Soil Science 43 (1), 52–58.

Ballantyne, A.K., 1968. Water-soluble salts in the parent material of Solonetzic and Chernozemic soils in Saskatchewan. Canadian Journal of Soil Science 48 (1), 43–48.

Ballantyne, A.K., 1978. Movement of salts in agricultural soils of Saskatchewan 1964 to 1975. Canadian Journal of Soil Science 58 (4), 501–509.

Chang, C., Oosterveld, M., 1981. Effects of long-term irrigation on soil salinity at selected sites in southern Alberta. Canadian Journal of Soil Science 61 (3), 497–505.

Chen, Z., Grasby, S.E., Osadetz, K.G., 2004. Relation between climate variability and groundwater levels in the upper carbonate aquifer, southern Manitoba, Canada. Journal of Hydrology 290 (1–2), 43–62.

Chudinova, S.M., Frauenfeld, O.W., Barry, R.G., Zhang, T., Sorokovikov, V.A., 2006. Relationship between air and soil temperature trends and periodicities in the permafrost regions of Russia. Journal of Geophysical Research 111 (F2), F02008, doi:10.1029/2005JF000342.

Clayton, J.S., Ehrlich, W.A., Cann, D.B., Day, J.H., Marshall, I.B., 1977. Soils of Canada. In: Soil Report, vol. 1. Canada Department of Agriculture, Ottawa.

Corwin, D.L., Lesch, S.M., Oster, J.D., Kaffka, S.R., 2006. Monitoring management-induced spatio-temporal changes in soil quality through soil sampling directed by apparent electrical conductivity. Geoderma 131 (3–4), 369–387.

Corwin, D.L., Sorensen, M., Rhoades, J.D., 1989. Field-testing of models which identify soils susceptible to salinity development. Geoderma 45 (1), 31–64.

Currie, R.G., 1984. Periodic (18.6-year) and cyclic (11-year) induced drought and flood in western North America. Journal of Geophysical Research 89 (D5), 7215–7230.

Currie, R.G., O'Brien, D.P., 1990. Deterministic signals in precipitation in the northwestern United States. Water Resources Research 26 (7), 1649–1656.

Danilov, D.L., Zhigljavsky, A.A. (Eds.), 1997. Principal Components of Time Series: The "Caterpillar" Method. St. Petersburg University Press, St. Petersburg (in Russian).

Eilers, R.G., Eilers, W.D., Fitzgerald, M.M., 1997. A salinity risk index for soils of the Canadian prairies. Hydrogeology Journal 5 (1), 68–79.

Elsner, J.B., Tsonis, A.A., 1996. Singular Spectrum Analysis: a New Tool in Time Series Analysis. Plenum Press, New York.

Fitzgerald, M.M., Eilers, R.G., 1999. Salinity assessment monitoring and prediction system (SAMPS). Benchmark site documentation: Warren, Manitoba. Land Resource Unit, Agriculture and Agri-Food Canada, Winnipeg.

Gan, T.Y., 1998. Hydroclimatic trends and possible climatic warming in the Canadian prairies. Water Resources Research 34 (11), 3009–3015.

Geonics Limited, 2005. EM38 ground conductivity meter operating manual. Geonics Limited, Mississauga.

Golyandina, N.E., Nekrutkin, V.V., Zhigljavsky, A.A., 2001. Analysis of Time Series Structure: SSA and Related Techniques. Chapman and Hall/CRC, London.

Grasby, S.E., Betcher, R.N., 2002. Regional hydrogeochemistry of the carbonate rock aquifer, southern Manitoba. Canadian Journal of Earth Sciences 39 (7), 1053–1063.

Greenlee, G.M., Pawluk, S., Bowser, W.E., 1968. Occurrence of soil salinity in the dry lands of southwestern Alberta. Canadian Journal of Soil Science 48 (1), 65–75.

Halvorson, A.D., 1990. Management of dryland saline seeps. In: Tanji, K.K. (Ed.), Agricultural Salinity Assessment and Management. American Society of Civil Engineers, New York.

Harker, D.B., Penner, L.A., Harron, W.R., Wood, R.C., MacDonald, D., 1996. Dryland salinity trends and indicators on the prairies. In: Proceedings of the Soil Quality Assessment for the Prairies Workshop, Jan. 22–24, 1996, Edmonton, Canada.

Henry, J.L., Bullock, P.R., Hogg, T.J., Luba, L.D., 1985. Groundwater discharge from glacial and bedrock aquifers as a soil salinization factor in Saskatchewan. Canadian Journal of Soil Science 65 (4), 749–768.

Heuvelink, G.B.M., Webster, R., 2001. Modelling soil variation: past, present, and future. Geoderma 100 (3–4), 269–301.

Keller, C.K., van der Kamp, G., 1988. Hydrogeology of two Saskatchewan tills: II. Occurrence of sulfate and implications for salinity. Journal of Hydrology 101 (1–4), 123–144.

Laio, F., Porporato, A., Ridolfi, L., Rodriguez-Iturbe, I., 2002. On the seasonal dynamics of mean soil moisture. Journal of Geophysical Research 107 (D15), 4272, doi:10.1029/2001JD001252.

Lesch, S.M., Herrero, J., Rhoades, J.D., 1998. Monitoring for temporal changes in soil salinity using electromagnetic induction techniques. Soil Science Society of America Journal 62 (1), 232–242.

MacDonald, G.M., Case, R.A., 2000. Biological evidence of multiple temporal and spatial scales of hydrological variation in the western interior of Canada. Quaternary International 67 (1), 133–142.

Menziani, M., Pugnaghi, S., Vincenzi, S., Santangelo, R., 2003. Soil moisture monitoring in the Toce valley (Italy). Hydrology and Earth System Sciences 7 (6), 890–902.

Miller, G.R., Baldocchi, D.D., Law, B.E., Meyers, T., 2007. An analysis of soil moisture dynamics using multi-year data from a network of micrometeorological observation sites. Advances in Water Resources 30 (5), 1065–1081.

Miller, J.J., Pawluk, S., 1994. Genesis of Solonetzic soils as a function of topography and seasonal dynamics. Canadian Journal of Soil Science 74 (2), 207–217.

Molchanov, A.M., 1967. Possible role of oscillating processes in evolution. In: Frank, G.M. (Ed.), Oscillating Processes in Biological and Chemical Systems. Nauka, Moscow (in Russian).

Mondal, M.K., Bhuiyan, S.I., Franco, D.T., 2001. Soil salinity reduction and prediction of salt dynamics in the coastal ricelands of Bangladesh. Agricultural Water Management 47 (1), 9–23.

Rhoades, J.D., Chanduvi, F., Lesch, S., 1999. Soil Salinity Assessment: Methods and Interpertation of Electrical Conductivity Measurements. FAO, Rome.

Richards, L.A. (Ed.), 1954. Diagnosis and Improvement of Saline and Alkali Soils. USDA, Washington.

Saunders, I.A., Byrne, J.M., 1994. Annual and seasonal climate and climatic changes in the Canadian prairies simulated by the CCC GCM. Atmosphere–Ocean 32 (3), 621–642.

Seybold, C.A., Mersie, W., Huang, J., McNamee, C., 2002. Soil redox, pH, temperature, and water-table patterns of a freshwater tidal wetland. Wetlands 22 (1), 149–158.

Soil Classification Working Group, 1998. The Canadian System of Soil Classification, third ed. NRC Research Press, Ottawa.

Stolte, W.J., Barbour, S.L., Eilers, R.G., 1992. Mechanisms influencing salinity development around prairie sloughs. Transactions of the American Society of Agricultural Engineers 35 (3), 795–800.

Van der Kamp, G., Maathuis, H., 1991. Annual fluctuations of groundwater levels as a result of loading by surface moisture. Journal of Hydrology 127 (1–4), 137–152.

Wagenet, R.J., 1998. Scale issues in agroecological research chains. Nutrient Cycling in Agroecosystems 50 (1–3), 23–34.

Wollenhaupt, N.C., Richardson, J.L., Foss, J.E., Doll, E.C., 1986. A rapid method for estimating weighted soil salinity from apparent soil electrical conductivity measured with an aboveground electromagnetic induction meter. Canadian Journal of Soil Science 66 (2), 315–321.

Woods, S.A., Hingley, L.E., 2004. Effects of frozen soil on electromagnetic inductance. In: Proceedings of the 41st Annual Alberta Soil Science Workshop, Feb. 17–19, 2004, Lethbridge, Canada.